



Shock tube study of the rate constants for $\text{H} + \text{O}_2 + \text{M} \rightarrow \text{HO}_2 + \text{M}$ ($\text{M} = \text{Ar}, \text{H}_2\text{O}, \text{CO}_2, \text{N}_2$) at elevated pressures

Jiankun Shao*, Rishav Choudhary, Adam Susa, David F. Davidson,
Ronald K. Hanson

Department of Mechanical Engineering, Stanford University, Stanford, CA 94305, United States

Received 21 November 2017; accepted 18 May 2018

Available online xxx

Abstract

The rate constants for the reaction $\text{H} + \text{O}_2 + \text{M} \rightarrow \text{HO}_2 + \text{M}$ were investigated at elevated pressures from 12 to 33 atm using ignition delay time (IDT) measurements behind reflected shock waves in $\text{H}_2/\text{O}_2/\text{M}$ mixtures with different collision partners $\text{M} = \text{Ar}, \text{H}_2\text{O}, \text{N}_2$ and CO_2 . The temperature and pressure ranges where the rate constants of the reactions $\text{H} + \text{O}_2 + \text{M} \rightarrow \text{HO}_2 + \text{M}$ and $\text{H} + \text{O}_2 \rightarrow \text{OH} + \text{O}$ dominate the IDT sensitivity were selected as optimum test conditions using the detailed H_2/O_2 mechanism of Hong et al. (2011). The current study thus provides a quantitative and relatively direct method for determining the rate constants for $\text{H} + \text{O}_2 + \text{M} \rightarrow \text{HO}_2 + \text{M}$ using simple IDT measurements. The rate constants found are consistent with earlier studies, but with reduced uncertainties.

© 2018 The Combustion Institute. Published by Elsevier Inc. All rights reserved.

Keywords: High pressure; Shock tube; Ignition delay time hydroperoxyl radical rate constant

1. Introduction

The reaction



is recognized as important in hydrocarbon combustion because of its role in chain branching, and the rate constant of this reaction has been extensively studied [1,2,3]. The reaction



directly competes with R1 by consuming H radical and generating relatively stable HO_2 radicals. This consumption is increased at elevated pressures and when there are efficient collision partners in the combustion system, such as H_2O and CO_2 . The competition between these two reaction channels, R1 and R2, strongly influences combustion phenomena in a wide variety of systems as R1 is an endothermic, and strongly temperature-dependent, chain-branching reaction, while R2 is an exothermic, weakly temperature-dependent, radical-terminating reaction. Their direct competition

* Corresponding author.

E-mail address: jkshao@stanford.edu (J. Shao).

suggests that the reaction rate constant of **R2** may be inferred from global properties, for example, ignition delay time (IDT), of hydrogen oxidation systems under conditions where the two reactions compete strongly and the rate constant for **R1** is sufficiently well-known.

Many past studies of the rate constant of **R2**, $k_{2,M}$, were limited to low temperatures, even though the reaction is more important in combustion devices at substantially higher temperatures. Surprisingly, there have been relatively few studies of $k_{2,M}$ at high temperatures in the literature, and only limited data for different collision partners. In the studies that have been performed, three main approaches were used.

The first approach is based on measurements of NO_2 in $\text{H}_2/\text{O}_2/\text{NO}$ systems. Ashmore and Tyler [4] proposed adding small quantities of NO_x to simplify the kinetic behavior of the system by providing an alternate consumption route for HO_2 radicals. Mueller et al. [5] and Bromly and Barnes [6] increased the NO_x concentration to enable **R3**, $\text{H} + \text{NO}_2 \rightarrow \text{NO} + \text{OH}$, to compete effectively with **R2** for H atoms. In this case, a steady-state analysis of the NO_2 and HO_2 concentrations provides a simple expression for k_2 ($[\text{NO}_2]_{ss} = k_2[\text{O}_2]/k_3$). Using the characteristic feature of the $\text{H}_2/\text{O}_2/\text{NO}_x$ systems, Bromly and Barnes estimated k_2 at 1 atm over a temperature range of 700–825 K using a flow reactor. Ashman and Haynes [7] used a laminar flow reactor for the temperature range 750–900 K and a pressure of 1 bar. Mueller et al. used the same method but at elevated pressures, 10–14 atm, and temperatures of 800–900 K. Subsequently, Bates et al. [8], in our laboratory, pushed this method to higher temperatures and different collision partners. They studied k_2 at temperatures between 1050 and 1250 K and pressures from 7 to 152 atm with bath gases of Ar, N_2 and H_2O behind reflected shock waves.

The second approach is based on measurement of species time-histories in oxidation systems. Getzinger et al. [9,10] used this method to measure k_2 . With the assumption that partial equilibrium is a valid approximation during recombination between 1150 and 1850 K in near stoichiometric mixtures, k_2 was inferred using OH absorption profiles. Blair and Getzinger [11] also monitored the growth of infrared emission at $2.7 \mu\text{m}$ from water vapor formed during the shock-initiated combustion of dilute $\text{H}_2/\text{O}_2/\text{Ar}$ systems to determine k_2 . Finally, Davidson et al. [12] used laser absorption measurements of OH time-histories and detailed kinetic modeling to improve the accuracy of this method.

A third approach, used in this study, is based on measurements of IDT, and was originally used by Slack [13]. This is effectively a direct approach to determine $k_{2,M}$ by matching measured ignition times with kinetic model simulations. Two common concerns with this approach are the effect of impu-

rities on the measured rates and the proper identification of the experimental test conditions where the IDT values are strongly sensitive to only two rate constants: k_1 and $k_{2,M}$. In the present study we have addressed these two concerns. Using laser absorption measurements, we are able to quantify and minimize the amount of impurities in our shock tube experiments [14]. As well, in the current study, experimental test conditions were identified by a systematic sensitivity analysis to determine the restricted temperature window where the two reactions **R1** and **R2** compete most strongly and dominate the overall kinetics.

The present study was performed at pressures of 17–33 atm. Notably, in the study by Bates et al. [8], no significant pressure dependence of k_2 was seen or expected below 80 atm. This observation is consistent with the current study that did not show any pressure dependence of k_2 over the test pressure range. The current measurements are thus effectively measurements of $k_{2,M}$ in the low pressure limit, i.e. $k_{2,0}$.

2. Experimental setup

The current IDT experiments were performed using the Stanford high-purity, high-pressure shock tube (HPST). The stainless steel driven section has an internal diameter of 5 cm and was heated to 90 °C. Diaphragms were made of aluminum or steel (with cross-scribing of different depths) to allow measurements over a broad range of pressure (17–33 atm). In this facility, typical uniform test times (for non-reactive synthetic air mixtures) were of the order of 2 ms when helium was used as the driver gas. High-purity hydrogen, oxygen, nitrogen and carbon dioxide gases were supplied by PraxairTM. Ultrapure water was generated using a SynergyTM UV water system, and a freeze-pump-thaw method was used to evacuate dissolved air before inducing the water vapor into the mixing tank. Gas mixtures were prepared manometrically in a 12.8-l stainless-steel mixing tank at 110 °C, and mixtures were stirred using a magnetically-driven vane assembly for at least 15 min prior to each experiment.

For each experiment involving water loading, the water concentration was measured in situ using a scanned-wavelength laser absorption method with a laser centered at 3920.089 cm^{-1} [23] and scan range of 1.5 cm^{-1} . The overall water loading measurement uncertainty was less than 3% and was included in the overall uncertainty of the current measurements. A sidewall-mounted KistlerTM PZT was located HPST 1.1 cm away from the shock tube end wall and provided pressure time-histories. The IDT is defined as the time interval between the arrival of the reflected shock and the onset of ignition determined by extrapolating the maximum slope of pressure signals back to the baseline. The same IDT definition was used for the

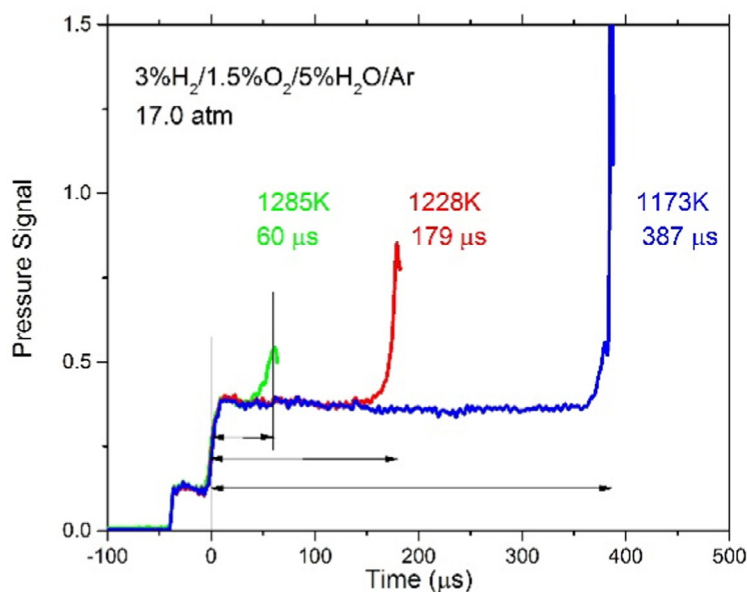


Fig. 1. Example ignition delay time measurements for 3% H_2 /1.5% O_2 /5% H_2O /Ar mixtures.

constant volume simulations. Representative ignition data from the shock tube are shown in Fig. 1. A slight pressure gradient before ignition was observed in Fig. 1, and the uncertainty caused by this was included in the overall uncertainty. The pressure profiles in the ignition experiments were not significantly affected by fuel loading as the mixtures were highly diluted.

3. Results and discussion

In this section, the reaction rate constants for $\text{H} + \text{O}_2 + \text{M} \rightarrow \text{HO}_2 + \text{M}$ with different collision partners are reported. In the first section, the reaction rate constant of $\text{H} + \text{O}_2 + \text{Ar} \rightarrow \text{HO}_2 + \text{Ar}$ is discussed and compared with earlier literature, and an improved rate constant correlation is given by combining the current measurements and selected literature values. Then, the reaction rate constants with other collision partners were determined as rate constant ratios with Ar. For each gas mixture, the methodology of using IDT measurement to infer the reaction rate constant is first discussed, followed by sensitivity analyses to select the optimum test conditions. Finally, the measured rate constants are compared with literature values, and uncertainty quantification is discussed. All the measured values are reported in the supplementary material with quantified uncertainties.

3.1. Reaction rate constant of $\text{H} + \text{O}_2 + \text{Ar} \rightarrow \text{HO}_2 + \text{Ar}$

At certain test conditions, the IDT of a $\text{H}_2/\text{O}_2/\text{Ar}$ gas mixture is strongly sensitive to the

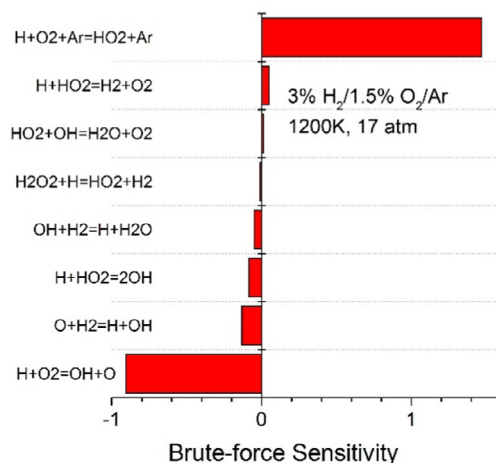


Fig. 2. Brute-force sensitivity analysis of IDT for a 3% H_2 /1.5% O_2 /Ar mixture at 1200 K, 17 atm.

rate constants k_1 and $k_{2,\text{Ar}}$. This implies an opportunity to use IDT measurements to infer the target reaction rate constant. An example of the sensitivity analyses of IDT is given in Fig. 2, for the case of a 3% H_2 /1.5% O_2 /Ar mixture at 1200 K and 17 atm. Here, the brute-force sensitivity is defined as $\ln(\tau_{2k}/\tau_k)$. Note that the rate constants k_1 and $k_{2,\text{Ar}}$ dominate the sensitivity plot for IDT at this condition. Since the competing rate constant k_1 has been well characterized in the literature with small uncertainty [3], a measurement of IDT at these test conditions can be used to infer $k_{2,\text{Ar}}$. However, before applying the method over a larger temperature

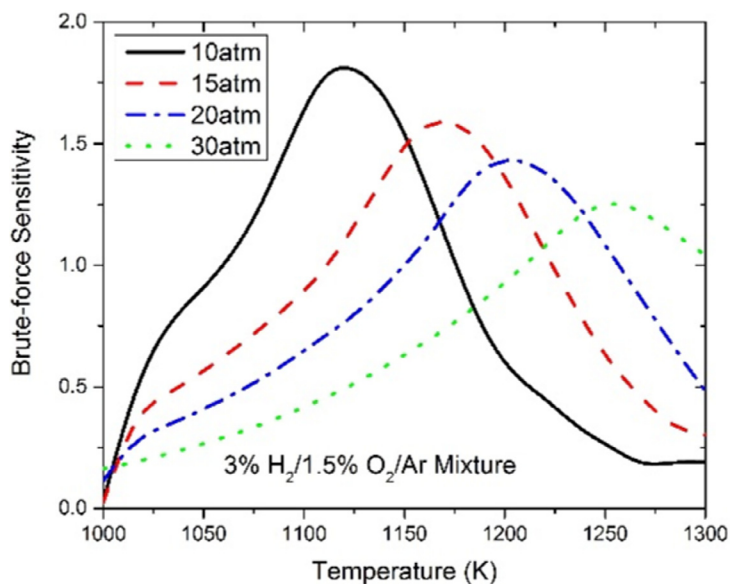


Fig. 3. Absolute sensitivity of $\text{H} + \text{O}_2 + \text{Ar} \rightarrow \text{HO}_2 + \text{Ar}$ reaction at different pressures for 3% H_2 /1.5% O_2 /Ar mixtures.

and pressure range, it is necessary to identify the temperature dependence of the sensitivity $k_{2,\text{Ar}}$ at each pressure.

Brute-force sensitivities for a range of temperatures and pressures for each test mixture were calculated using the Hong et al. mechanism [15]. Figure 3 shows the range based on the sensitivity analysis where the IDT is most sensitive to k_1 and $k_{2,\text{Ar}}$. The temperature range of peak sensitivity at each pressure is narrow and the peak moves to higher temperature with increased pressure. In this study, we chose only measurement conditions where the brute-force sensitivity value is larger than one. This limit is arbitrary, but provides a relatively small uncertainty tolerance.

Figure 4 presents the current $k_{2,\text{Ar}}$ data, the data from Bates et al. [8] and recommendations from Troe, Baulch et al. [16,17] and the recently released recommendations of Smith et al. [2] known as FFCM-1. Our dataset is relatively consistent with prior high-temperature data, of Bates et al. and Davidson et al., but note the reduced uncertainties of the current data.

Figure 5 shows a comparison of the current results with earlier literature studies. The best-fit to our measurements and past literature studies results is found to be $k_{2,\text{Ar}} = 2.6 \times 10^{-32} (T/300)^{-1.2} \text{ cm}^6 \text{ molecule}^{-2} \text{ s}^{-1}$. This rate constant correlation uses the same temperature dependence as Troe [16] and Bates et al. [8]. The absolute value is approximately higher 20–30% than the value given previously by Bates et al. [8] ($2.0 \times 10^{-32} (T/300)^{-1.2} \text{ cm}^6 \text{ molecule}^{-2} \text{ s}^{-1}$) and value suggested by Troe ($2.2 \times 10^{-32} (T/300)^{-1.2} \text{ cm}^6 \text{ molecule}^{-2} \text{ s}^{-1}$) [16].

3.2. Reaction rate constant of $\text{H} + \text{O}_2 + \text{M} \rightarrow \text{HO}_2 + \text{M}$ with other collision partners

Similar sensitivity analyses of IDT were also conducted for $\text{H}_2/\text{O}_2/\text{H}_2\text{O}/\text{Ar}$ mixtures. Due to the lower vapor pressure of water than other compositions, condensation may occur when preparing these mixtures. To avoid uncertainties related to water condensation, in situ laser absorption measurements were used to quantify the water concentration before each experiment. The measured water concentrations were used in the rate constant determinations and a $\pm 3\%$ water loading uncertainty was added to the total uncertainty of the measurements. The comparison of different uncertainty sources is also included in this section.

For the mixtures tested, $k_{2,\text{H}_2\text{O}}$, $k_{2,\text{Ar}}$, and k_1 are the dominant reactions in the sensitivity plot, as shown in Fig. 6. In the following determination of $k_{2,\text{H}_2\text{O}}$, the currently measured value of $k_{2,\text{Ar}}$ was used. As in the case with $\text{M} = \text{Ar}$, the sensitivities of the dominant reactions change with temperature and pressure. These trends were analyzed and the optimum test conditions determined. As with the $\text{H}_2/\text{O}_2/\text{Ar}$ mixture, the peak-temperature sensitive range changes with pressure. At low pressures, the peak of the sensitive range is located at a lower temperature, and the peak moves to a higher temperature at higher pressures. In this study, we chose conditions where the absolute sensitivity is larger than a certain limit. The limit is again arbitrary, but provides an acceptable uncertainty tolerance.

Results are shown in Fig. 7. The best fit to the data using the temperature dependence of Troe is $k_{2,\text{H}_2\text{O}} = 59.88 \times 10^{-32} (T/300)^{-1.2} \text{ cm}^6 \text{ molecule}^{-2}$

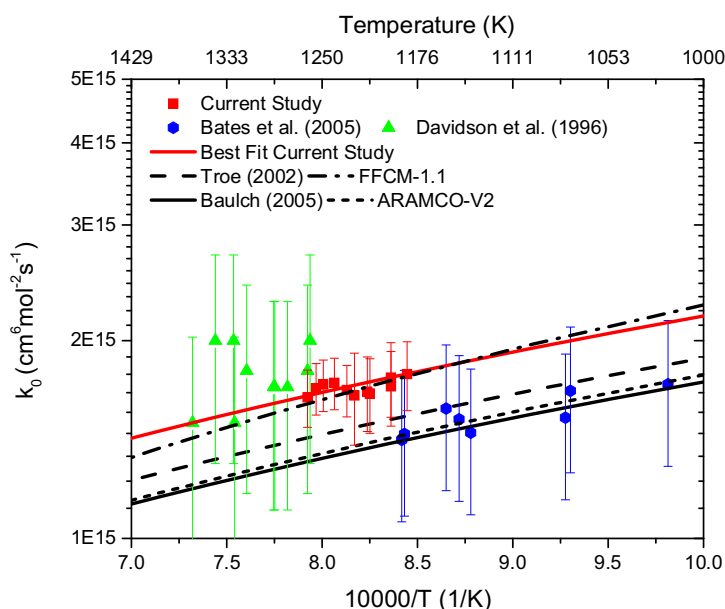


Fig. 4. Measured and recommended low pressure rate constants for $k_{2,\text{Ar}}$.

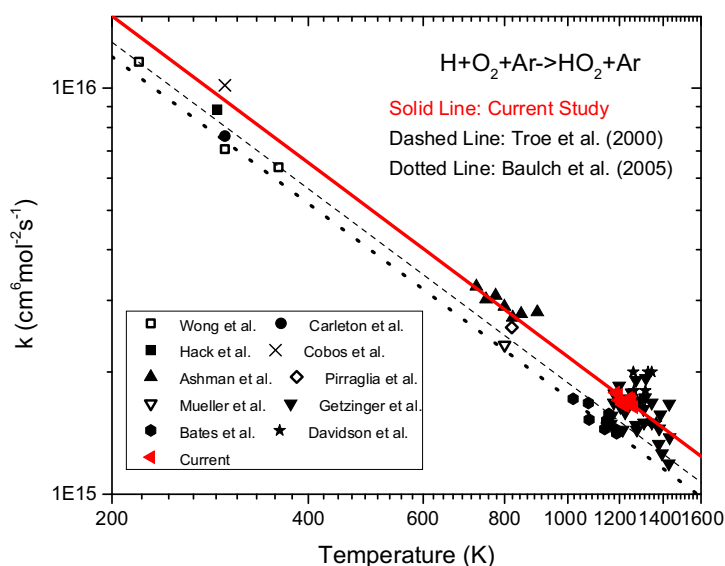


Fig. 5. The measured reaction rate constant $k_{2,\text{M}}$ of $\text{H} + \text{O}_2 + \text{Ar} \rightarrow \text{HO}_2 + \text{Ar}$ and the best fit rate constant [5,7,8,12,18–21].

s^{-1} . The measured collision efficiency ratio for water and argon $k_{2,\text{H}_2\text{O}}/k_{2,\text{Ar}} = 23.0$. This value is in close agreement with Bates et al. [8] ($k_{2,\text{H}_2\text{O}}/k_{2,\text{Ar}} = 22.4$ at 1200 K). Recommended values from the FFCM-1 mechanism [2] ($k_{2,\text{H}_2\text{O}}/k_{2,\text{Ar}} = 26.35$), and Baulch et al. [17] ($k_{2,\text{H}_2\text{O}}/k_{2,\text{Ar}} = 25.2$) are slightly higher. The value of Ash-

man and Haynes [7] ($k_{2,\text{H}_2\text{O}}/k_{2,\text{Ar}} = 19$) is 13% lower.

There are several sources of uncertainty in the current $\text{M} = \text{H}_2\text{O}$ measurements in addition to the uncertainties common to the $\text{M} = \text{Ar}$ experiments. The major uncertainty in $k_{2,\text{H}_2\text{O}}$ stems from the uncertainty in the $\text{M} = \text{Ar}$ measurement, $k_{2,\text{Ar}}$. Uncertainties in the reflected shock

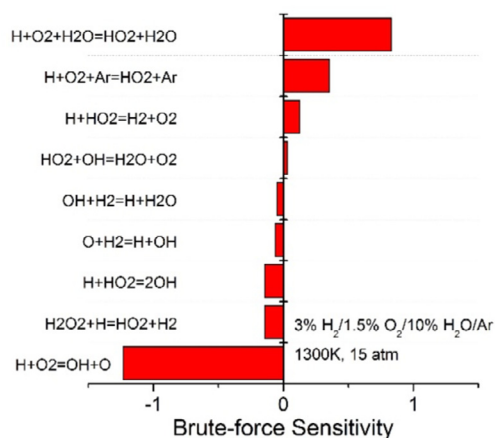


Fig. 6. Sensitivity analysis of 3% H_2 /1.5% O_2 /10% H_2O /Ar mixture at 1300 K, 17 atm.

temperature (± 10 K) are folded into the uncertainty of k_1 ($\pm 5\%$), which is the experimental parameter that shows the strongest variation with temperature. The uncertainty in the shock tube measurements of k_1 by Hong and others [3] includes the uncertainty in T_5 in the overall uncertainty of k_1 . The in situ laser absorption measurement of water loading significantly reduces its associated uncertainty ($\pm 3\%$). Initial impurities, represented by H-atoms, which at these temperatures typically do not exceed 0.01 ppm [14], can contribute as much as +5% to the $k_{2,\text{H}_2\text{O}}$ uncertainty. The uncertainty associated with the IDT determination increases with temperature because of

the uncertainty associated with the shorter values of IDT at high temperatures. The IDT measurement uncertainty assumed here is ± 5 μs , and this leads to $\pm 10\%$ uncertainty in $k_{2,\text{H}_2\text{O}}$ above 1300 K. Quantitatively determined overall 2σ uncertainties for the tested cases are included in the supplementary material.

The rate constants, k_{2,CO_2} and the reaction rate constants, k_{2,N_2} , for the reactions $\text{H} + \text{O}_2 + \text{M} \rightarrow \text{HO}_2 + \text{M}$ were determined using the same methodology. As before, the sensitivity analyses of IDT were first conducted for $\text{H}_2/\text{O}_2/\text{CO}_2/\text{Ar}$ and $\text{H}_2/\text{O}_2/\text{N}_2$ mixtures to determine the optimum test conditions

For the $\text{M} = \text{CO}_2$ rate constant determination, k_{2,CO_2} , $k_{2,\text{Ar}}$ and k_1 were the dominant reactions in the sensitivity analysis. As for the case with $k_{2,\text{H}_2\text{O}}$ the value of $k_{2,\text{Ar}}$ derived in the present study was used in determining k_{2,CO_2} . The sensitivities of the dominant reactions were again functions of temperature and pressure. Sensitivity analyses were conducted to select the temperature window of the test conditions. For example, the highest sensitivity temperature for the $\text{M} = \text{CO}_2$ determination at 10 atm was 1200 K and for 17 atm was 1275 K. It should be noted, in particular, that the reaction $\text{CO}_2 + \text{H} \rightarrow \text{CO} + \text{OH}$ had only an insignificant effect on the rate constant determination in the selected temperature window. IDT measurements were conducted for two mixtures, 3% H_2 /1.5% O_2 /20% CO_2 /Ar and 3% H_2 /1.5% O_2 /10% CO_2 /Ar, at two pressures, 10 atm and 17 atm. Results are shown in Fig. 8. The best fit to the data is $k_{2,\text{CO}_2} = 13.0 \times$

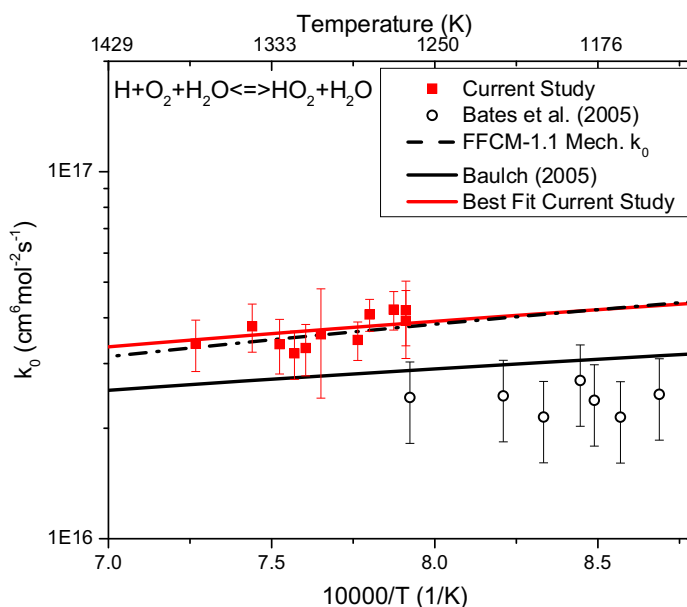


Fig. 7. The reaction rate constant $k_{2,\text{H}_2\text{O}}$ for the reaction $\text{H} + \text{O}_2 + \text{H}_2\text{O} \rightarrow \text{HO}_2 + \text{H}_2\text{O}$.

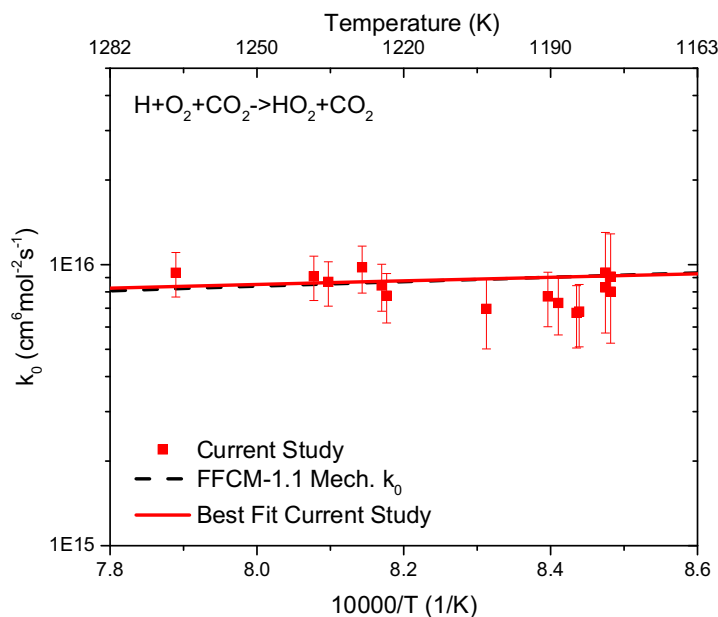


Fig. 8. The rate constant for $\text{H} + \text{O}_2 + \text{CO}_2 \rightarrow \text{HO}_2 + \text{CO}_2$ inferred using the current method.

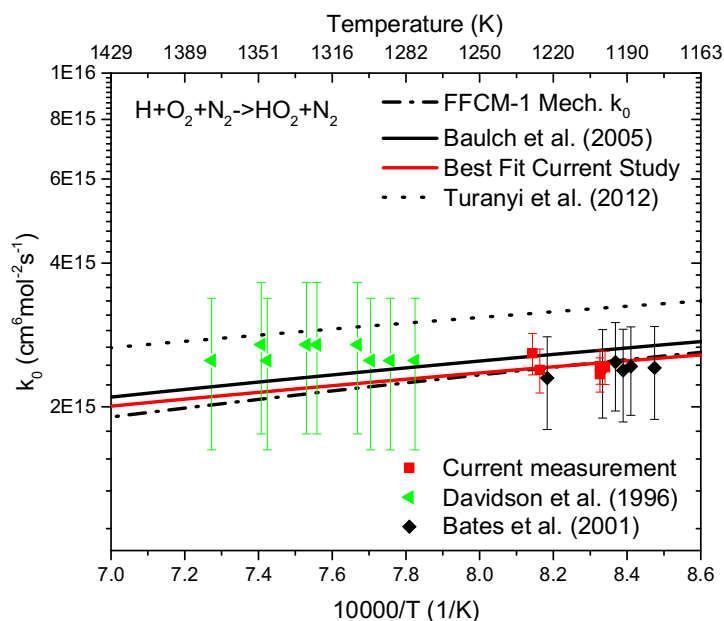


Fig. 9. The reaction rate constant for $\text{H} + \text{O}_2 + \text{N}_2 \rightarrow \text{HO}_2 + \text{N}_2$ inferred using the current method. [22].

$10^{-32}(T/300)^{-1.2} \text{ cm}^6 \text{ molecule}^{-2} \text{ s}^{-1}$. The FFCM-1 mechanism is in good agreement with the current study.

For the $\text{M} = \text{N}_2$, experiments, there was no argon in the mixture, thus k_{2,N_2} and k_1 were the only dominant reactions. IDT measurements conducted at 12 atm for the 3% H_2 /1.5% O_2 / N_2 mixture were used to infer k_{2,N_2} . Results are shown in Fig. 9.

The current data have significantly reduced uncertainty than in the Davidson et al. and Bates et al. studies. The best fit to the data is $k_{2,\text{N}_2} = 3.60 \times 10^{-32}(T/300)^{-1.2} \text{ cm}^6 \text{ molecule}^{-2} \text{ s}^{-1}$. The FFCM-1 mechanism and Baulch et al. are in good agreement with the current study.

In the Hong et al. mechanism [15], CO_2 and N_2 occur only as a collision partner in the

association reactions and were assumed not to participate in the H_2/O_2 kinetics. A comparison of the IDT values for the $\text{M} = \text{CO}_2$ experiments was made between the Hong et al. mechanism and the FFCM-1 mechanism [2] (which does include C/O chemistry) using the same values of k_1 and $k_{2,\text{Ar}}$ in both studies. Determinations of k_{2,CO_2} and k_{2,N_2} were effectively unchanged, supporting the assumption that this determination is robust against small mechanism variations.

4. Conclusion

The reaction rate constants of $\text{H} + \text{O}_2 + \text{M} \rightarrow \text{HO}_2 + \text{M}$ are studied at 12–33 atm for four different collision partners: Ar, N_2 , H_2O , and CO_2 . The measured rate constants are consistent with past literature while providing rate constants with reduced uncertainties. The determined rate constants for $\text{M} = \text{Ar}$ and H_2O are slightly higher than previous studies, but, by definition, provide excellent reproduction of high-pressure, low-temperature H_2/O_2 ignition delay time experiments when used in conjunction with the rate constant expression for k_1 derived from shock tube/laser absorption measurements [1–3].

Using the measurements of the present study, combined with the temperature dependence suggested by Troe [16], analytical representations of temperature and bath gas dependence of $k_{2,0}$ can be given. Overall 2σ uncertainties are based on averages of uncertainties listed in the supplementary material.

$$k_{2,0} [\text{M} = \text{Ar}] = 2.6 \times 10^{-32} (T/300)^{-1.2} \text{ cm}^6 \text{ molecule}^{-2} \text{ s}^{-1} (\pm 12\%)$$

$$k_{2,0} [\text{M} = \text{N}_2] = 3.6 \times 10^{-32} (T/300)^{-1.2} \text{ cm}^6 \text{ molecule}^{-2} \text{ s}^{-1} (\pm 12\%)$$

$$k_{2,0} [\text{M} = \text{CO}_2] = 13.0 \times 10^{-32} (T/300)^{-1.2} \text{ cm}^6 \text{ molecule}^{-2} \text{ s}^{-1} (\pm 24\%)$$

$$k_{2,0} [\text{M} = \text{H}_2\text{O}] = 59.8 \times 10^{-32} (T/300)^{-1.2} \text{ cm}^6 \text{ molecule}^{-2} \text{ s}^{-1} (\pm 19\%)$$

In this study, the measured collision efficiency ratio for water and argon $k_{2,\text{H}_2\text{O}}/k_{2,\text{Ar}} = 23.0$; the measured collision efficiency ratio for nitrogen and argon $k_{2,\text{N}_2}/k_{2,\text{Ar}} = 1.38$; the measured collision efficiency ratio for carbon dioxide and argon $k_{2,\text{CO}_2}/k_{2,\text{Ar}} = 5.0$;

Acknowledgments

This work was supported by the Air Force Office of Scientific Research through AFOSR Grant

No. FA9550-16-1-0195, with Chiping Li as contract monitor. (Development of HyChem – A Jet and Rocket Propellant Fuel Combustion Chemistry Model.)

Supplementary materials

Supplementary material associated with this article can be found, in the online version, at doi:10.1016/j.proci.2018.05.077.

References

- [1] S. Wang, D.F. Davidson, R.K. Hanson, *J. Phys. Chem. A* 121 (45) (2017) 8561–8568.
- [2] G.P. Smith, Y. Tao, H. Wang, “Foundational Fuel Chemistry Model Version 1.0 (FFCM-1),” <http://nanoenergy.stanford.edu/ffcm1>, 2016.
- [3] Z. Hong, D.F. Davidson, E.A. Barbour, R.K. Hanson, *Proc. Combust. Inst.* 33 (2011) 309–316.
- [4] P.G. Ashmore, B.J. Tyler, *Trans. Faraday Soc.* 58 (1962) 1108–1116.
- [5] M.A. Mueller, R.A. Yetter, F.L. Dryer, *Proc. Combust. Inst.* 27 (1998) 177–184.
- [6] J.H. Bromly, F.J. Barnes, P.F. Nelson, B.S. Haynes, *Int. J. Chem. Kinet.* 27 (1995) 1165–1178.
- [7] P.J. Ashman, B.S. Haynes, *Proc. Combust. Inst.* 27 (1998) 185–191.
- [8] R.W. Bates, D.M. Golden, R.K. Hanson, C.T. Bowman, *Phys. Chem. Chem. Phys.* 3 (2001) 2337–2342.
- [9] R.W. Getzinger, L.S. Blair, *Combust. Flame* 13 (1969) 271–284.
- [10] R.W. Getzinger, G.L. Schott, *J. Chem. Phys.* 43 (1965) 3237–3247.
- [11] L.S. Blair, R.W. Getzinger, *Combust. Flame* 14 (1970) 5–12.
- [12] D.F. Davidson, E.L. Petersen, M. Röhrig, R.K. Hanson, C.T. Bowman, *Proc. Combust. Inst.* 26 (1996) 481–488.
- [13] M.W. Slack, *Combust. Flame* 28 (1977) 241–249.
- [14] J. Urzay, N. Kseib, D.F. Davidson, G. Iaccarino, R.K. Hanson, *Combust. Flame* 161 (2014) 1–15.
- [15] Z. Hong, D.F. Davidson, R.K. Hanson, *Combust. Flame* 158 (2011) 633–644.
- [16] J. Troe, “Detailed modeling of the temperature and pressure dependence of the reaction $\text{H} + \text{O}_2 (+\text{M}) \rightarrow \text{HO}_2 (+\text{M})$,” *Proc. Combust. Inst.* 28 (2000) 1463–1469.
- [17] D.L. Baulch, C.T. Bowman, C.J. Cobos, et al., *J. Phys. Chem. Ref. Data* 34 (2005) 757–1397.
- [18] W. Wong, D.D. Davis, *Int. J. Chem. Kinet.* 6 (1974) 401–416.
- [19] W. Hack, *Berichte der Bunsengesellschaft für Phys. Chem.* 81 (1977) 1118–1119.
- [20] K.L. Carleton, W.J. Kessler, W.J. Marinelli, *J. Phys. Chem.* 97 (1993) 6412–6417.
- [21] C.J. Cobos, H. Hippler, J. Troe, *J. Phys. Chem.* 89 (1985) 342–349.
- [22] T. Turanyi, T. Nagy, I.G. Zsely, et al., *Int. J. Chem. Kinet.* 44 (2012) 284–302.
- [23] C.S. Goldenstein, I.A. Schultz, R.M. Spearrin, J.B. Jeffries, R.K. Hanson, *Applied Phys. B* 116 (3) (2014) 717–727.